Preparation and Mechanical Properties of Composite of Fibrous Cellulose and Maleated Polyethylene

FARAO ZHANG, TAKASHI ENDO, WULIN QIU, LIQUN YANG, TAKAHIRO HIROTSU

Institute for Marine Resources and Environment Research, National Institute of Advanced Industrial Science and Technology, 2217-14 Hayashi-Cho, Takamatsu 761-0395, Japan

Received 9 November 2000; accepted 27 August 2001

ABSTRACT: Fibrous cellulose and maleated polyethylene (FC–MPE) composites were prepared under melt mixing by maleation of polyethylene (PE) to obtain maleic anhydride (MA) grafted PE (MPE) and successive compounding of the resultant MPE with fibrous cellulose (FC). When increasing the content of added MA to 2 wt %, the grafting efficiency of MA decreases gradually to 84% and the grafted MA chains become longer. Scanning electron microscopy (SEM) reveals strong adhesion of MPE to FC in the FC–MPE composite, which is probably due to the increased compatibility between MPE and FC, in contrast to no adhesion of unmaleated PE (UPE) to FC in the FC–UPE composite. This difference in interfacial structure between the FC–MPE and FC–UPE composites results in quite different mechanical properties for them. With an increase in the FC content to 60 wt %, the tensile strength of the FC–MPE composite increases significantly and reaches 125% that of pure PE. Furthermore, the larger Young's modulus, larger bending elastic modulus, and smaller elongation of the FC–MPE composite strongly indicate effective transfer of the high tensile strength and elasticity of FC to the MPE matrix through the strong adhesion between FC and MPE. © 2002 Wiley Periodicals, Inc. J Appl Polym Sci 84: 1971–1980, 2002; DOI 10.1002/app.10428

Key words: polyethylene; composites; compatibility; mechanical properties

INTRODUCTION

Extensive utilization of cellulose has attracted growing interest,[1–2] because of its high specific strength, good thermal stability, and particularly its massive reproducibility and environmental benefits compared with synthetic polymers derived from petroleum. However, cellulose exhibits no thermoplasticity because of the tight inter- and intramolecular hydrogen bonding; thus, its applications have been essentially limited to only a few areas such as paper and rayon. Compounding of cellulose with a synthetic polymer is undoubtedly a good alternative to develop new materials with the advantageous properties of the constituents.

A cellulose–polyethylene (PE) composite is expected to be a promising candidate, because PE is the most widely used synthetic polymer, cellulose is the most abundant natural polymer on the earth, and the excellent thermoplasticity of PE may compensate for the disadvantagously poor processability of cellulose with rigid molecular chains. A key problem exists in the method of preparation of a composite with good mechanical properties.

Many studies have been carried out on polymer composites reinforced by cellulose, in which cellulose is a minor component used as a reinforcer and synthetic polymers such as polypropylene

Correspondence to: T. Hirotsu (takahiro-hirotsu@aist.go.jp).

Contract grant sponsor: National Institute of Advanced Industrial Science and Technology, Japan.

Journal of Applied Polymer Science, Vol. 84, 1971–1980 (2002)

© 2002 Wiley Periodicals, Inc.

(PP),[4–11] PE,[12–14] and others[15–20] are the main component forming a matrix. The compatibility or interfacial adhesion, which improves the dispersion of cellulose and the transfer of stress from one phase to the other, has been generally considered to determine the final properties of the composite. Several methods, coating or pretreatment of fibers[5–7,8,11,15,17,18] and chemical modification of the matrix,[4,9,10,14] have been reported for improving the interfacial compatibility between hydrophilic cellulose and hydrophobic polymers. Grafting of maleic anhydride (MA) on PE or PP is the most effective method for improving the interfacial adhesion of cellulose and a PE or PP matrix, because of the formation of covalent bonds through esterification between MA groups and hydroxyl groups of cellulose.[6,7,9,21]

In this study we investigate the maleation of PE and compounding of the resultant maleated PE (MPE) with cellulose under melt mixing to prepare composites of fibrous cellulose and MPE (FC–MPE) with FC contents of 5–60 wt %. The mechanical properties of the FC–MPE composite are discussed in regard to the relation of the content of MA groups in the MPE and the content of FC in the composite.

EXPERIMENTAL

Materials

The FC was purchased from Whatman International Co., Ltd. The density of the FC was measured as 1.53 g/cm^3. The PE (pellets, high density of 0.95 g/cm^3) was a commercially available grade (grade 7000F, Mitsui Sekiyu Kagaku). The MA, dehydrated acetone, and xylene were procured from Wako Chemicals and benzoyl peroxide (BPO, Nacalai Tesque), all of which were reagent grade, were used without further purification.

Methods

Maleation of PE

The PE pellets were mechanically milled into spherical grains with a size of about 1 mm before maleation. The MA and BPO as an initiator were sequentially dissolved in dehydrated acetone, and the acetone solution (100 g/L MA, 8 g/L BPO) was then sprayed onto the PE powder. Four PE mixtures containing 0.25, 0.5, 1, and 2 wt % MA were vacuum dried at 25°C for 2 h to evaporate the acetone solvent. The maleation of each dried PE mixture was performed in a melt mixer with a chamber volume of 60 cm^3 (30C150 Labo Plastomill, Toyo Seiki) at 200°C and 90 rpm for 10 min to prepare MA-grafted PE (MPE$_n$; n = 0.25, 0.5, 1, or 2 wt %).

Purification of MPE

Crude MPE (3 g) was heated in 300 mL of xylene (130°C, 6 h), and then about 800 mL of cold acetone was added to the hot solution of MPE. The precipitated MPE was filtered, washed with acetone at 75°C in a Soxhlet extractor for 24 h, and finally vacuum dried at 50°C for 24 h.

Chemical Titration

Purified MPE (1 g) was dissolved in 200 mL of xylene (130°C, 3 h). The hot solution was titrated with a 0.1*M* isopropanolic KOH solution using five drops of a 1% thymol blue dimethylformamide solution as an indicator. After a color change to blue, the solution was backtitrated with a 0.1*M* isopropanolic HCl solution to the yellow end point. The MA content (wt %) was calculated according to the following equation:

$$\mathrm{MA} = 0.49 \times (V_{\mathrm{KOH}} - V_{\mathrm{HCl}})$$

where V_{KOH} and V_{HCl} are the volumes (mL) of the KOH and HCl solutions added, respectively.

Preparation of FC–MPE Composites

The FC was vacuum dried at 50°C for 14 days before compounding with MPE. The FC–MPE composites were prepared in the mixer described above. First a mixture (37.5 g) of FC and MPE was preheated at 165°C for 1 min in the mixer, and then FC was compounded with the melted MPE at 200°C and 90 rpm for 10 min. After the compounding, the composite was taken out and shaped into small pellets (<5 mm). Composites of FC and unmaleated PE (FC-UPE) were also prepared by the same method for comparison.

Sheet and Film Preparation

Sheets and films of MPE and FC–MPE composites were prepared by a compression-molding method. Their thicknesses were adjusted by using middle frames with different thicknesses. Pellets of MPE and FC–MPE composites were heat pressurized at 190°C and 10 MPa for 4 min using a SFA-37 automatic molding press (Shinto Metal

Ind. Ltd.) with an automatic cycle of heating, pressurizing, and cooling. Teflon films were used to avoid direct contact between the MPE and FC–MPE composites and the stainless surface of the mold.

Tensile Test

Tensile tests were carried out according to JIS K7113 for the testing method of tensile properties of plastics.[22] The sheet samples were conditioned at 20°C and 65% relative humidity for 24 h in a controlled environment room before measuring the tensile properties with a tensile tester (AG-100A, Shimadzu) at a strain speed of 50 mm/min.

Dynamic Mechanical Analysis (DMA)

The DMA of the composites was performed with a Perkin–Elmer DMA 7e analyzer using a three-point bending rectangular measuring system. The size of the rectangular samples was 20 × 5 × 1 mm (length × width × thickness). Indium and ice were used for temperature calibration of the apparatus. The measurements were carried out under a 550-mN static force and a 500-mN dynamic force at 1-Hz frequency and a temperature scanning rate of 5°C/min.

FTIR Spectroscopy

Films of 10–100 μm thickness were used for FTIR measurements. The FTIR spectra were recorded on a Spectrum 2000 spectrometer (Perkin–Elmer Co., Ltd.) with a resolution of 4 cm^{-1} in the spectral range of 4000–500 cm^{-1}.

Observation by Scanning Electron Microscopy (SEM)

The fractures of the FC–MPE composites after tensile tests were coated with a thin gold–palladium layer and observed with a Hitachi S-2460N scanning electron microscope.

RESULTS AND DISCUSSION

Maleation of PE

It has been reported that the maleation of PE by a radical reaction in a melt state generally proceeds through the following steps: formation of radicals by the decomposition of initiators, abstraction of hydrogen atoms from the molecular chains of PE by radicals, grafting of MA monomers on macroradicals of PE, and a termination reaction by a combination of radicals. Accordingly, we should also consider the possibilities of the crosslinking of PE chains and the homopolymerization of MA monomers in the maleation of PE.

Figure 1 shows the IR spectra of MPEs. In contrast to UPE, all the MPEs exhibit a new absorption band at around 1790 cm^{-1} that is due to the symmetric C=O stretching vibration of grafted MA groups on the background of PE, and there is no absorption band at 1780 cm^{-1} because of free MA [Fig. 1(a)].[23] As seen in the magnified spectrum [Fig. 1(b)], the intensity of the absorption band at around 1790 cm^{-1} increases with an increase in the amount of added MA monomers, indicating an increase in the content of MA groups on the PE. Further, the position of the absorption band shifts to a lower wavenumber from 1792 to 1788.5 cm^{-1}, implying the formation of longer grafted groups of MA or free poly(MA) (PMA) in MPE. We carefully examined the IR spectra of MPEs purified by dissolving the crude MPEs in xylene, followed by precipitation with acetone [Fig. 1(c)]. Nongrafted PMA and MA monomers dissolved into the acetone phase are removed from the precipitate of MPE. There is no difference in the position of the characteristic absorption band between the crude and the purified MPEs. This strongly suggests that almost all of the MA monomers are grafted on the PE and the length of the grafted chains increases with an increase in the amount of added MA and initiator in the order $MPE_{0.25}$ (= one MA unit) ≈ $MPE_{0.5}$ < MPE < MPE_2. Weak bands at 1715 cm^{-1} indicate the hydrolysis of a slight amount of MA groups grafted on the PE.[23]

The dissolution of MPE in xylene yielded no insoluble gels. This indicates that significant crosslinking of PE chains hardly occurs in the present maleation of PE. There is a weight loss from MPE after purification (Table I). This implies that MPE contains acetone-soluble impurities, which are probably due to the initiator and very slight traces of nongrafted monomers and polymers of MA. We determined the amount of grafted MA groups in MPE from the titration of purified MPE. Table I shows that the content of grafted MA groups in MPE is proportional to the amount of added MA monomers, and the grafting efficiency is larger than 84%. Accordingly, the contents of MA groups in $MPE_{0.25}$, $MPE_{0.5}$, MPE_1, and MPE_2 are 0.23, 0.47, 0.85, and 1.68 wt %, respectively.

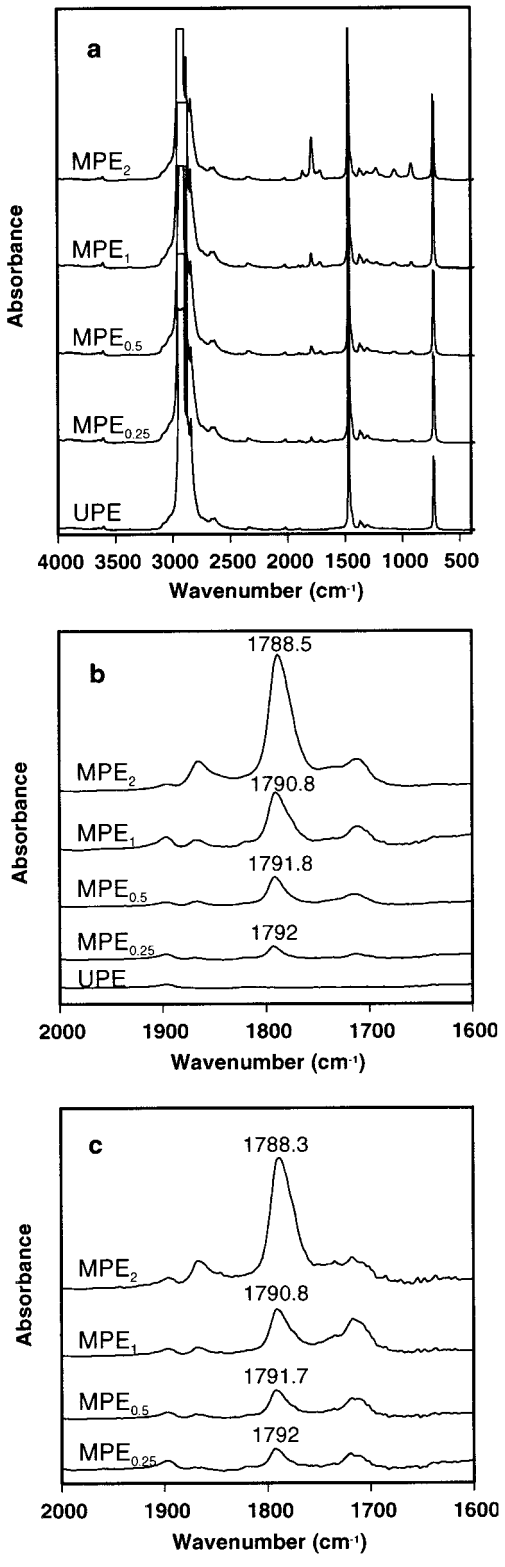

Figure 1 IR spectra of unmaleated PE (UPE) and maleated PE (MPE): (a,b) crude and (c) purified MPE.

Interfacial Adhesion and Microstructure

The SEM observations show that the average length and diameter of FC are about 300 and 20 μm, respectively (Fig. 2). FC has a crystallinity of 93% and a crystal structure of the native cellulose type I.[3] Figure 3 shows IR spectra of FC–UPE and FC–MPE composites with a cellulose content of 15 wt %. The spectral pattern of cellulose is little changed by the compounding with UPE and MPE [Fig. 3(a)]. Furthermore, the characteristic absorption band of grafted MA groups at around 1790 cm^{-1} still exists in the FC–MPE composites [Fig. 3(b)]. This result indicates that the compounding of cellulose with MPE barely yields the formation of ester bonds between the OH groups of cellulose and the MA groups of MPE, which is quite different from the case when compounding chlorella and MPE.[21] The very low reactivity between MPE and cellulose is probably attributable to the extremely decreased number of free OH groups on the FC, because of the high crystallinity[3] and large size of the FC (Fig. 2).

The SEM images of fractures of FC–UPE and FC–$MPE_{0.25}$ composites with FC contents of 5, 30, and 60 wt % are shown in Figure 4(a–c), respectively. For the composites with 5 wt % FC, strong adhesion is clearly observed between $MPE_{0.25}$ and FC [Fig. 4(a-2)], but there is no adhesion between UPE and FC [Fig. 4(a-1)]. Similar differences in adhesion are observed for the composites with FC contents of 30 and 60 wt % shown in Figure 4(b,c), respectively. The FC–$MPE_{0.5}$, FC–MPE_1, and FC–MPE_2 composites also exhibited microstructures similar to that of the FC–$MPE_{0.25}$ composite.

The densities of FC–$MPE_{0.25}$ and FC–UPE composites with 60 wt % FC were measured as

Table I Maleation of PE

Sample	Weight Loss after Purif. (%)	Content of MA Groups in Purified MPE (wt %)	Content of MA Groups in MPE (wt %)	Grafting Efficiency (%)
UPE	0.3	0	0	
$MPE_{0.25}$	0.4	0.23	0.23	91.6
$MPE_{0.5}$	0.85	0.47	0.47	93.2
MPE_1	1.13	0.86	0.85	85
MPE_2	1.49	1.71	1.68	84

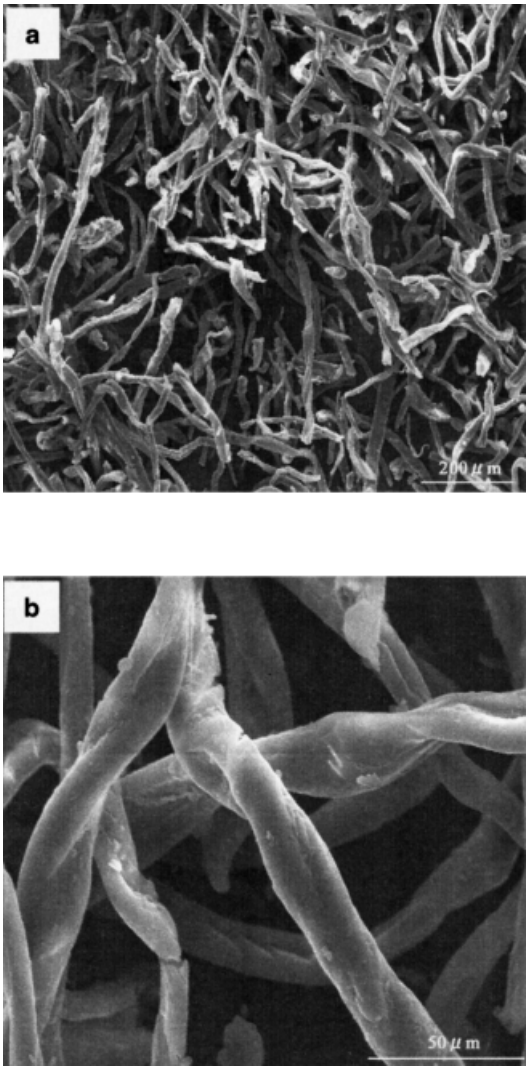

Figure 2 SEM micrographs of cellulose with (a) an average length of about 300 μm and (b) an average width of about 20 μm.

1.20 and 1.08 g/cm^3, respectively, which are lower than the theoretical density of 1.30 g/cm^3 that is based upon the weight fractions and densities of the FC and PE components. The decrease in density implies the existence of air gaps in the composites, which probably locate mainly in the interface between the FC and PE phases. The lower density is quite consistent with the larger air gaps for the FC–UPE composite, compared with the FC–MPE composite. Assuming that air gaps exist only in the interfaces between the FC and PE phases and evenly cover the cellulose fibers (20-μm diameter, 300-μm length) like a cylindrical wall, the average thickness of the air gaps in composites with 60 wt % FC can be estimated to be 0.83 μm for the FC–MPE composite and 1.92 μm for the FC–UPE composite (see Appendix I). Similarly, the sizes of the air gaps for the other FC–UPE composites with FC contents of 5–30 wt % were estimated to be close to 1.92 μm.

The tighter contact between MPE and FC for the FC–MPE composite is probably due to the more increased compatibility of MPE with FC. This adhesion results in a quite different microstructure for the FC–MPE composites than that for the FC–UPE composite. A small difference in the microstructure between FC–MPE composites may indicate a marked enhancement of the adhesion between FC and MPE by a small amount of MA groups in the MPE.

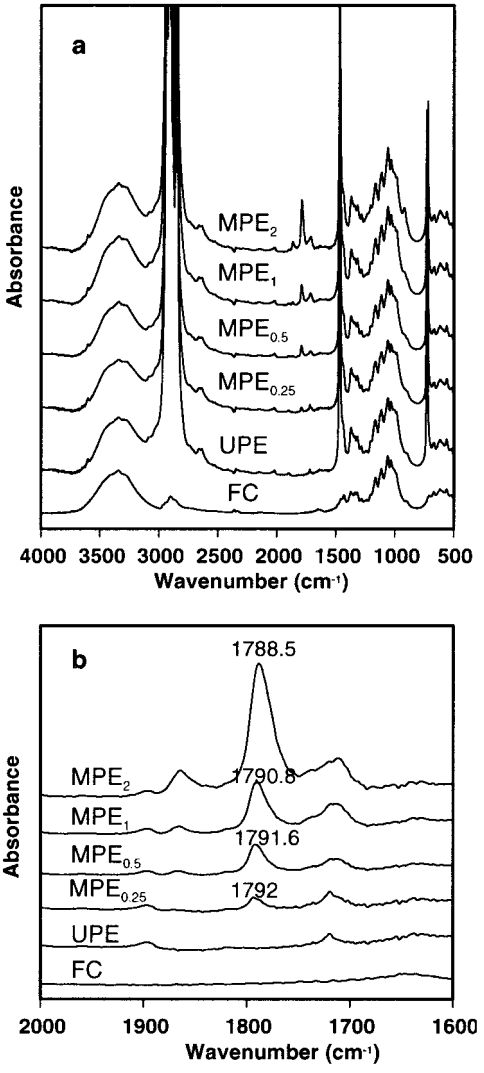

Figure 3 (a) IR spectra of cellulose and the composites containing 15 wt % cellulose and 85 wt % PE matrices and (b) the magnified spectra.

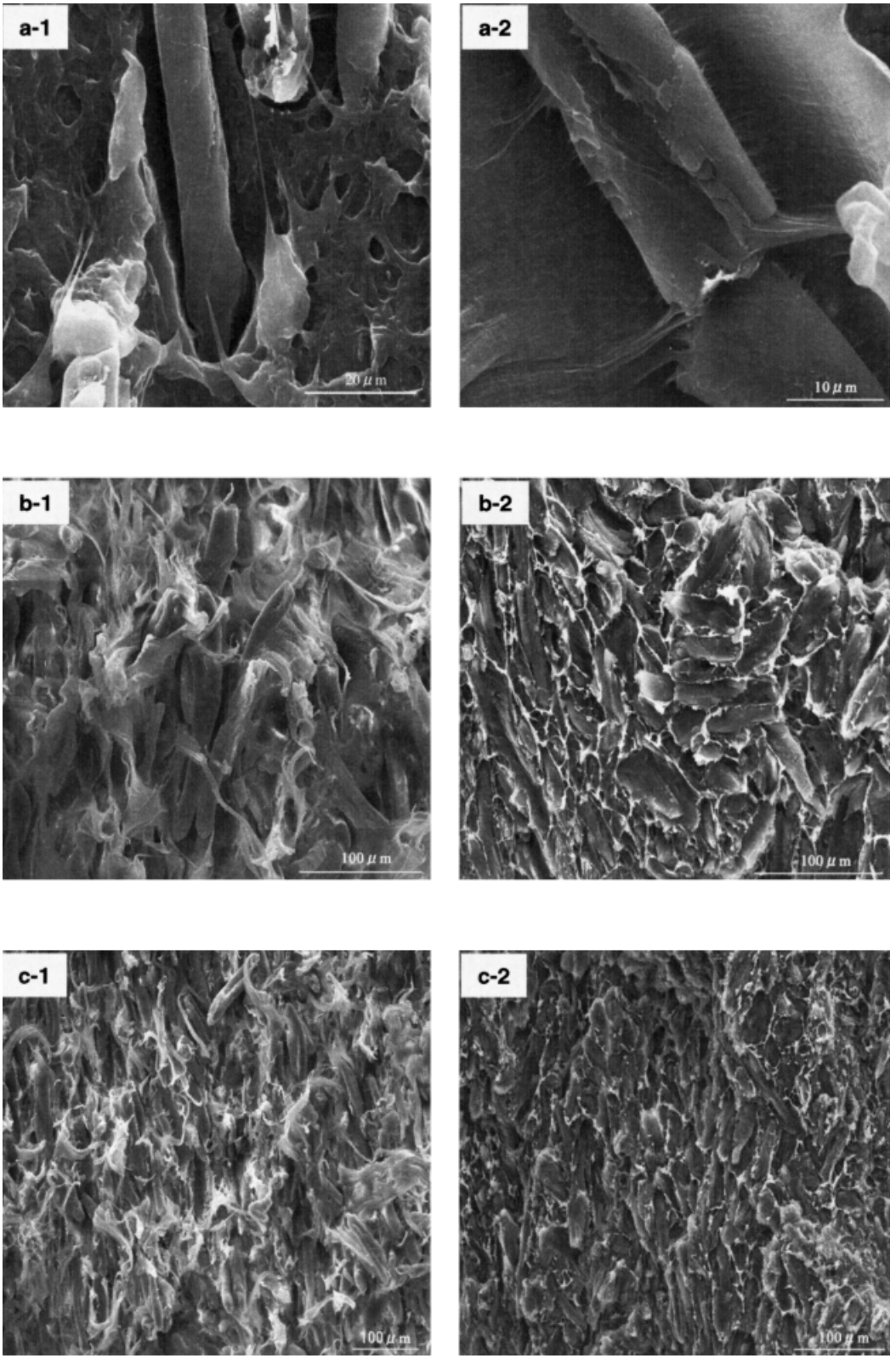

Figure 4 SEM micrographs of the composites of 5 wt % cellulose with (a-1) UPE and (a-2) $MPE_{0.25}$ matrices, 30 wt % cellulose with (b-1) UPE and (b-2) $MPE_{0.25}$ matrices, and 60 wt % cellulose with (c-1) UPE and (c-2) $MPE_{0.25}$ matrices.

Mechanical Properties

Stress–strain curves of FC–UPE and FC–MPE composites containing 5, 30, and 60 wt % FC are shown in Figure 5. The elongation of the composites decreases significantly with an increase of the cellulose content. For the composites containing 5 wt % FC [Fig. 5(a)], the FC–UPE and FC–MPE composites exhibit almost the same tensile strength but different elongations and toughnesses. Increasing the FC content above 5 wt % causes the tensile strength of the FC–MPE composite to increase much more than that of the FC–UPE composite. Regardless of the FC content range from 5 to 60 wt %, the FC–$MPE_{0.5}$ composite exhibits the best tensile properties, although even a smaller amount of MA groups in MPE (0.23 wt % for $MPE_{0.25}$) is effective enough to produce a satisfactory effect. Thus, the tensile strength of FC–MPE composites containing 60 wt % FC reaches 125% that of 100% PE (Table II).

The viscoelasticity of the composites was investigated by DMA. The elasticity is evaluated from the storage modulus, which is defined as

$$(\sigma_\phi/\varepsilon_\phi)\cos\,\delta,$$

where σ_ϕ is the amplitude of dynamic stress, ε_ϕ is the amplitude of strain, and δ is the phase lag between the stress and the strain. Figure 6 shows the storage moduli of FC–UPE and FC–$MPE_{0.25}$ composites with different FC contents. The storage moduli of the composites increase with the FC content, which is a good reflection of the rigid nature of cellulose. Little difference in the storage modulus is observed between the FC–UPE and FC–MPE composites when the FC content is below 30 wt %, while a large difference appears at an FC content of 60 wt %. The viscoelasticity of the composites with an FC content of 60 wt % was then examined using different matrixes (Fig. 7). As for the storage modulus [Fig. 7(a)], the FC–UPE composite exhibits the lowest value while the FC–MPE composites exhibit values nearly equal to each other. Referring to the corresponding tan δ [i.e., the ratio of the viscosity to the elasticity, Fig. 7(b)], the FC–UPE composite has a larger value than the FC–MPE composites, which have almost the same values as each other.

The bending strain increases with an increase in the temperature. The FC–UPE composite exhibited a slightly larger bending strain than the FC–MPE composites, for example, a static strain of 3% and a dynamic strain of 0.07% for the FC–

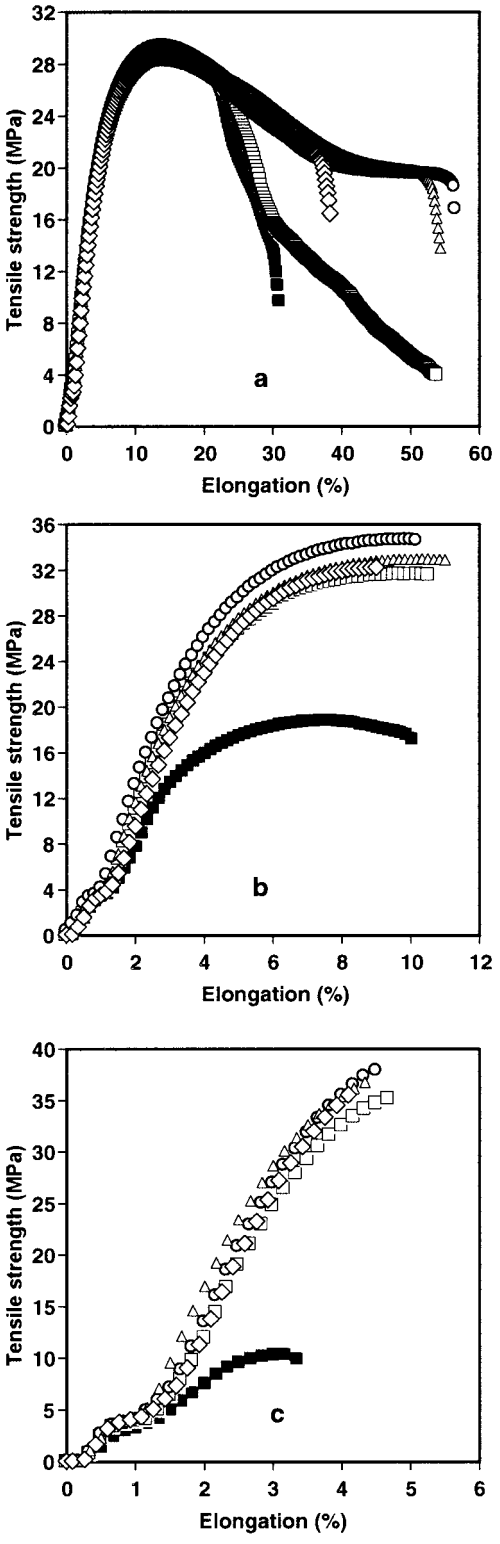

Figure 5 The tensile properties of the composites containing (a) 5, (b) 30, and (c) 60 wt % cellulose with different matrices of (■) UPE, (□) $MPE_{0.25}$, (○) $MPE_{0.5}$, (△) MPE_1, and (◇) MPE_2.

Table II Tensile Properties of FC–MPE Composites

FC Content (wt %)	Matrix	Tensile Strength (MPa)	Young's Modulus (GPa)	Elongation (%)
0	UPE	28.6	0.54	
	$MPE_{0.25}$	28.9	0.54	
	$MPE_{0.5}$	28.9	0.54	
	MPE_1	28.3	0.53	
	MPE_2	29.6	0.57	
5	UPE	28.5	0.63	31
	$MPE_{0.25}$	29.4	0.6	59.4
	$MPE_{0.5}$	29.5	0.61	56.8
	MPE_1	28.6	0.58	62.8
	MPE_2	28.9	0.59	38.6
15	UPE	28.4	0.75	11.3
	$MPE_{0.25}$	30.7	0.71	16.7
	$MPE_{0.5}$	31.1	0.72	23.7
	MPE_1	30.9	0.7	19.7
	MPE_2	30.8	0.72	17.7
30	UPE	18.4	0.63	9.1
	$MPE_{0.25}$	32.9	0.93	9.0
	$MPE_{0.5}$	34.1	0.95	10.7
	MPE_1	33.0	0.92	10.9
	MPE_2	32.3	0.84	9.0
60	UPE	10.5	0.54	3.0
	$MPE_{0.25}$	35.2	0.99	4.4
	$MPE_{0.5}$	37.5	1.03	4.4
	MPE_1	36.9	1.42	4.1
	MPE_2	36.5	0.96	4.1

UPE composite versus a static strain of 2.5–2.8% and a dynamic strain of 0.04–0.06% for the FC–MPE composites. Because the total strains of all the composites are larger than 2.5%, we can estimate a bending strain larger than 25 μm for samples with a thickness of 1 mm.

The mechanical properties of FC–UPC and FC–MPE composites can be explained by their different microstructures as described earlier. Strong adhesion between the FC and MPE phases is observed for the FC–MPE composites, and little adhesion between FC and UPE phases is revealed with larger air gaps in the interface. The efficiency of the transfer of tensile stress in the composites is largely determined by the structure of the interface between the FC and MPE or UPE.[21] Thus, we can expect that the efficiency of the transfer of tensile stress in the FC–MPE composite is much higher than that in the FC–UPE composite. This explains that the tensile strength of the FC–MPE composite increases with an increase in the FC content, because the tensile strength of FC is greater than that of MPE; conversely, the tensile strength of the FC–UPE composite decreases with an increase in the FC content because of little contribution from the FC phase.

On the other hand, the efficiency of the transfer of bending stress in the composites is probably dependent on the size of the air gaps in the interface between the FC and MPE or UPE phases. If the bending strain is larger than the size of air gaps, the bending stress loading on the composite can be effectively transferred to the cellulose fibers. The bending strain (>25 μm) is much larger than the size of the air gaps (around 1.92 μm) for the FC–UPE composite. Accordingly, the storage modulus of the composite can increase with an increase in the FC content because of the higher

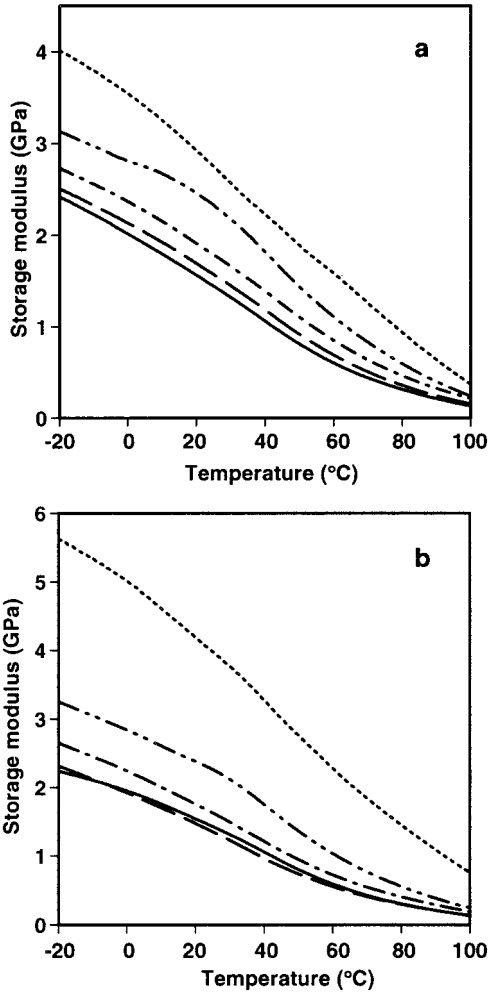

Figure 6 Plots of the storage modulus versus the temperature of the composites of (a) UPE and (b) $MPE_{0.25}$ with (—) 0, (- - -) 5, (- · -) 15, (- · · -) 30, and (· · ·) 60 wt % cellulose.

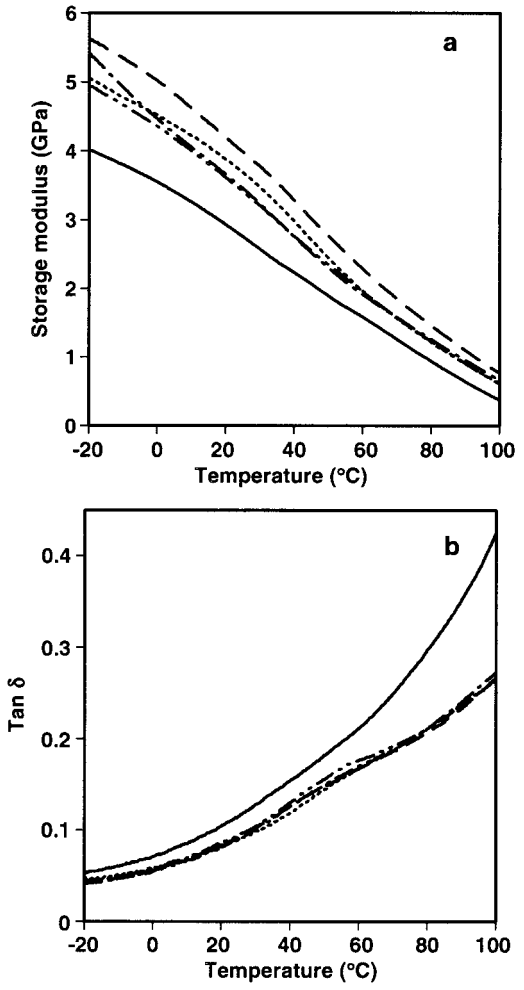

Figure 7 Plots of the (a) bending storage modulus and (b) tan δ versus the temperature of the composites with 60 % cellulose and 40 wt % (—) UPE, (- - -) $MPE_{0.25}$, (- · -) $MPE_{0.5}$, (- · · -) MPE_1, and (· · ·) MPE_2.

elastic modulus of FC. This agrees with the increases in the storage modulus of the FC–UPE and FC–MPE composites with an increase in the FC content shown in Figure 6. The lower storage modulus of the FC–UPE composite than that of the FC–MPE composite at the FC content of 60 wt % may be due to the rougher dispersion of FC in the UPE matrix with increasing FC content. The similarity in the mechanical properties of the FC–MPE composites with different contents of MA groups is due to the similarity in the microstructure among the composites.

CONCLUSION

A FC–MPE composite with good mechanical properties can be prepared under melt mixing by maleation of PE and successive compounding of the resulting MPE with FC. Even a slight maleation of PE results in good adhesion of MPE to FC, which enables the stress to be efficiently transferred from the MPE to FC phases. Thus, the composite exhibits increased tensile strength and elastic modulus with an increase in the FC content.

APPENDIX I

Assuming no air gaps in the interface between the FC and PE phases in an ideal FC–PE composite, we can obtain the following equations:

$$V_I d_I = V_{FC} d_{FC} + V_{PE} d_{PE} \quad (A.1)$$

$$V_I = V_{FC} + V_{PE} \quad (A.2)$$

where the V_I and d_I are the volume and density of the ideal composite, respectively, the values of which can be calculated from the weight fractions and densities of the FC and PE components; V_{FC} and d_{FC} are the volume and density of the FC, respectively; and V_{PE} and d_{PE} are the volume and density of the PE matrix, respectively. Further, if we assume that air gaps exist only in the interface between the FC and PE phases and cylindrically encapsulate cellulose fibers with a constant thickness (r) for a practical FC–PE composite, the following relations are satisfied:

$$V_P d_P = V_{FC} d_{FC} + V_{PE} d_{PE} \quad (A.3)$$

$$V_P = V_{FC} + V_{AG} + V_{PE} \quad (A.4)$$

and

$$V_{AG}/V_{FC} = \{\pi(R_1 + r)^2 - \pi R_1^2\}/\pi R_1^2 \quad (A.5)$$

where V_P and d_P are the volume and density of the practical FC–PE composite, respectively; V_{AG} is the volume of air gaps; and R_1 is the radius of FC. Thus, we can estimate the average thickness of the air gaps around FC (r) for the FC–UPE and FC–MPE composites with 60 wt % FC from eq. (A.5) using theoretical and experimental data: d_I = 1.30 g/cm^3, d_{PE} = 0.95 g/cm^3, d_{FC} = 1.53 g/cm^3, R_1 = 10 μm, and $(V_{FC}d_{FC})/(V_{PE}d_{PE})$ = 6/4.

REFERENCES

1. Endo, T.; Zhang, F.; Kitagawa, R.; Hirotsu, T.; Hosokawa, J. Polym J 2000, 32, 182.
2. Endo, T.; Kitagawa, R.; Zhang, F.; Hirotsu, T.; Hosokawa, J. Chem Lett 1999, 1155.
3. Endo, T.; Kitagawa, R.; Hirotsu, T.; Hosokawa, J. Kobunshi Ronbunshu 1999, 56, 166.
4. Collier, J. R.; Lu, M.; Fahrurrozi, M.; Collier, B. J. J Appl Polym Sci 1996, 61, 1423.
5. Coutinho, F. M. B.; Costa, T. H. S.; Carvalho, D. L. J Appl Polym Sci 1997, 65, 1227.
6. Joly, C.; Kofman, M.; Gauthier, R. J Macromol Sci Pure Appl Chem 1996, A33, 1981.
7. Felix, J. M.; Gatenholm, P. J Appl Polym Sci 1991, 42, 609.
8. Bataille, P.; Ricard, L.; Sapieha, S. Polym Compos 1989, 10, 103.
9. Karnani, R.; Krishnan, M.; Narayan, R. Polym Eng Sci 1997, 37, 476.
10. Belgacem, M. N.; Bataille, P.; Sapieha, S. J Appl Polym Sci 1994, 53, 379.
11. Sain, M. M.; Kokta, B. V. J Appl Polym Sci 1993, 48, 2181.
12. Kim, T.-J.; Lee, Y.-M.; Im, S.-S. Polym Compos 1997, 18, 273.
13. Bataille, P.; Allard, P.; Cousin, P.; Sapieha, S. Polym Compos 1990, 11, 301.
14. Hedenberg, P.; Gatenholm, P. J Appl Polym Sci 1996, 60, 2377.
15. Gatenholm, P.; Bertilsson, H.; Mathiasson, A. J Appl Polym Sci 1993, 49, 197.
16. Vieira, A.; Nunes, R. C. R.; Visconti, L. L. Y. Polym Bull 1996, 36, 759.
17. Maldas, D.; Kokta, B. V.; Raj, R. G.; Daneault, C. Polymer 1988, 29, 1255.
18. Felix, J. M.; Gatenholm, P. Polym Compos 1993, 14, 449.
19. Garcia-Ramirez, M.; Cavaille, J. Y.; Dupeyre, D.; Peguy, A. J Polym Sci Polym Phys 1994, 32, 1437.
20. Garcia-Ramirez, M.; Cavaille, J. Y.; Dupeyre, D.; Peguy, A. J Polym Sci Polym Phys 1995, 33, 2109.
21. Zhang, F.; Kabeya, H.; Kitagawa, R.; Hirotsu, T.; Yamashita, M; Otsuki, T. Chem Mater 1999, 11, 1952.
22. Japan Standard Society. JIS K7113–1995 Testing Method for Tensile Properties of Plastics; Japan Standard Society: Tokyo, 1995.
23. De Roover, B.; Sclavons, M.; Carlier, V.; Devaux, J.; Legres, R.; Momtaz, A. J Polym Sci Polym Chem 1995, 33, 829.